

# Two dimensional liquid phase separations of proteins using online fractionation and concentration between chromatographic dimensions

Jonathan A. Karty, William E. Running, James P. Reilly\*

Department of Chemistry, Indiana University, Bloomington, IN 47405, USA

Received 7 April 2006; accepted 21 September 2006

Available online 23 October 2006

## Abstract

Multi-dimensional liquid chromatography is often presented as an alternative to two-dimensional (2-D) gel electrophoresis for separating complex protein mixtures. The vast majority of analytical-scale 2-D LC systems have employed either off-line fractionation or stepped gradients in the first dimension separation. The latter severely restrict flexibility in setting up the first dimension gradient. We propose a novel two-dimensional LC system that employs online fractionation of proteins into a series of small reversed phase trapping columns. These traps effectively decouple the two separation dimensions and avoid problems associated with off-line fraction collection. Flexibility in determining the gradient programs for the two separations is thus enhanced. The reduced diameter of the trapping columns concentrates analyte between chromatographic dimensions. The apparatus is coupled with online electrospray time-of-flight mass spectrometry to characterize ribosomal proteins of *Caulobacter crescentus*. © 2006 Elsevier B.V. All rights reserved.

**Keywords:** Multidimensional chromatography; 2-D LC; Proteomics; Sample preparation

## 1. Introduction

The rapidly evolving discipline of proteomics provides unique insights into the machinery of living cells. However, the complexity of biological systems places unique demands on analytical methodology. Genomes contain several thousand genes (e.g. [1–4]), each encoding a different protein and those gene products can undergo a wide variety of chemical modifications after translation. (e.g. [5–17]) Furthermore, proteins are not all present in equal amounts, and their concentrations vary in response to developmental and environmental stimuli (e.g. [18]). Coupling these complexities with the practical limitations on the number of analytes that any detector can simultaneously observe makes separation science a central concern in all proteomic methodologies.

Although two-dimensional (2-D) gel electrophoresis is the most widely used technique for the separation of complex protein mixtures, it has several well-documented disadvantages [19–26]. Multi-dimensional liquid chromatography is often sug-

gested as an alternative to 2-D gels for separating complex protein mixtures (reviewed in [21,27–29]). The most basic form of 2-D liquid chromatography involves off-line fraction collection from one separation column and injection of those fractions onto a second column with different separation chemistry (e.g. ion exchange and reversed phase). Several variations of this methodology have been presented in the literature including preparative isoelectric focusing followed by non-porous reversed phase chromatography, [30–33] off-line chromatofocusing-non-porous C<sub>18</sub> LC–MS [34–36] strong anion exchange-hydrophobic interaction chromatography [37], and injecting strong cation exchange (SCX) fractions into a multiplexed reversed phase LC–MS system [38]. Off-line fractionation is not an ideal solution, however. Sample evaporation and/or contamination can occur between dimensions and it is very difficult to completely transfer the fractions to the second separation. An improved system would be sealed against the environment and would ensure complete transfer of the first dimension fractions into the second separation stage.

A handful of online fractionation methods have been described in the literature. Opticek and coworkers have constructed several multi-dimensional LC systems [39–41], including one featuring size-exclusion chromatography (SEC) followed by reversed phase LC–MS [41]. The proteins eluting

\* Corresponding author at: 800 E. Kirkwood Ave., Bloomington, IN 47405, USA. Tel.: +1 812 855 1980; fax: +1 812 855 8300.

E-mail address: [reilly@indiana.edu](mailto:reilly@indiana.edu) (J.P. Reilly).

from the size exclusion column were adsorbed onto one of two polystyrene divinylbenzene reversed phase (RP) columns attached to a column switching valve. A 4 min reversed gradient was performed with the column not in line with the SEC column. The 240 min SEC gradient was divided into 60 fractions by alternating which RP column was placed in line with the SEC column. Wagner et al. designed a multidimensional LC apparatus combining a restricted access media ion-exchanger, an analytical ion exchange column, and four non-porous C<sub>18</sub> columns [42] dividing a 96 min ion exchange separation into 24 different fractions each analyzed with an 8 min reversed phase gradient. Liu et al. devised a similar system combining strong cation exchange and C<sub>4</sub> RP chromatographies [43]. The SCX column was developed with a stepped gradient, which eluted the proteins onto one of two C<sub>4</sub> columns. LC–MS data were recorded for 10 SCX fractions. Similar stepped ion-exchange, dual reversed phase column systems have been used for multidimensional LC–MS–MS of complex peptide mixtures (e.g. [40,44,45]). Chen et al. employed six trapping columns and a pair of column selection valves to fractionate peptides from a capillary isoelectric focusing experiment [46]. The traps effectively decoupled the first and second dimensions, circumventing the time constraints encountered in the columns-in-series systems described previously while avoiding the problems associated with off-line fraction collection. The timescales of the second dimension gradients in the systems described by Opticek et al. and Wagner et al. were determined by their respective first dimension separations. That is, the second dimension separations had to take significantly less time than the first dimension separations. Improved results might be obtained if the gradients for two separations were independent of each other.

The columns in the different dimensions of the protein separation systems described above had nearly the same inner diameter (i.d.) and both separations were performed at approximately the same flow rate. Short reversed phase columns have been used for years to capture peptides from liquid streams prior to capillary scale liquid chromatography (e.g. [45,47–49]) allowing relatively high flow rates (2–20  $\mu\text{L}/\text{min}$ ) for loading samples into chromatography systems that normally operate at less than 1  $\mu\text{L}/\text{min}$ . The 2-D LC system described in the present work makes use of short, reversed phase trapping columns to capture proteins as they elute from an ion exchange column developed with a linear gradient. The trapping and second dimension columns are of significantly smaller inner diameter than the first dimension column, thus concentrating analytes between dimensions. The traps decouple the two separation dimensions, desalt, and concentrate the analytes in a single step.

## 2. Strategy of apparatus

A handful of fundamental design questions needed to be addressed during the development of this system. The first was how much of a size differential between the two columns was feasible. For maximum sensitivity, one might couple a preparative scale first dimension column (>7 mm i.d.) with a capillary scale second dimension (<100  $\mu\text{m}$  i.d.). However, the total system pressure required to flow several mL/min of solvent through

an extremely narrow capillary packed with small particles would exceed the capacities of standard HPLC fittings; a modest difference in diameters is more feasible. Furthermore, small i.d. columns have very limited loading capacities. Fortunately, one trap need not be capable of handling all of the protein loaded into the first dimension column; it only captures the proteins in a single fraction. In this work, the effluent from a 4.6 mm i.d. column is fractionated into a series of 1.0 mm i.d. traps.

Another major design question was whether storing proteins on trapping columns for extended periods of time (in excess of 50 h for the 60-trap system described below) incurs a significant degradation in the performance of the second dimension separation. It was hoped that adsorption to the stationary phase would minimize diffusion during the time between separations. If the proteins diffused excessively during the intervening time, they would elute as very broad peaks, and the resolution of the second separation would be very poor. Furthermore, the resolution of the second separation might vary depending on how long proteins were adsorbed to a particular trap.

The final major design question concerned the number of reversed phase analytical columns employed by the final apparatus. There are three basic strategies for the reversed phase dimension of the two-dimensional separation. The first is to employ no additional analytical column, i.e. use the trapping columns themselves for the second dimension; this arrangement is not commonly employed. A single analytical column placed between the trap and mass spectrometer is a simple and economic approach, but the time spent re-equilibrating the analytical column between the reversed phase separations can become excessive. Several researchers employ two or more second dimension analytical columns to avoid this problem [29,41,43]. Usually the analytical columns are placed on a multi-port switching valves in an arrangement that allows one column to equilibrate while a separation gradient is applied to another. There are two complications with this setup, however. The first is the cost and complexity of the additional columns, valve, and pumps. The second is that it is nearly impossible to obtain two or more perfectly matched HPLC columns. Even if two columns are well matched when new, their characteristics will likely diverge as they age. Thus, a species may elute from the two columns at slightly different retention times, frustrating comparisons between multiple analyses. Similar problems are encountered when comparing multiple two-dimensional gel electrophoresis experiments (i.e. the same protein may appear in slightly different positions on a 2-D gel depending on running conditions, sample loading, etc.). These questions and others are explored.

## 3. Experimental

### 3.1. Instrument overview

The automated two-dimensional liquid chromatograph system consisted of an array of Valco Cheminert multiport valves (VICI Inc., Houston, TX) controlled by micro-electric actuators. All connections between elements of the apparatus were made with 127  $\mu\text{m}$  i.d., 1.59 mm outer diameter PEEK tubing

(red PEEK, Upchurch Scientific, Oak Harbor, WA) to minimize the volumes between elements. The performance of this system was assessed by separating samples of ribosomal proteins from *Caulobacter crescentus* bacteria.

### 3.2. Sample preparation

Ribosomes were chosen because they provide sufficient complexity (54 proteins) to characterize the resolving power of the separations while being simple enough (i.e. all proteins present in nearly equimolar amounts, sequences well-annotated in genome) for the mass spectra to be readily interpreted with a minimum of data processing. Samples of tightly coupled *C. crescentus* ribosomes were prepared according to the procedure described by Spedding [50]. The ribosomes were disassociated and the ribosomal RNA removed according to the protocol of Hardy et al. [51]. Protein concentrations in the extracts were estimated by Bradford dye binding assay [52]. The four proteins used in the initial system tests and were purchased from Sigma (St. Louis, MO).

### 3.3. Chromatographic conditions

All two-dimensional separations described in this paper used strong cation exchange columns for the first dimension separation and C<sub>4</sub> reversed phase columns for the second. The first dimension column was a 4.6 mm i.d. × 35 mm long TSKGel SP-NPR non-porous SCX (sulfopropyl) column (Tosoh Biosep LLC, Montgomeryville, PA) chosen to handle the back pressure incurred as solvents passed through the both the ion exchange column and the trapping columns. The effluent from the first dimension was directed into a series of 1.0 mm i.d. × 20 mm long Javelin guard columns packed with 5 μm Biobasic C<sub>4</sub> media (ThermoHypersil Keytone, Bellafonte, PA). The second dimension separation occurred on one of two 1.0 mm i.d. × 75 mm long Pioneer analytical columns packed with Biobasic C<sub>4</sub> placed after the traps. The first dimension gradient was created by a Waters 2695 liquid chromatograph (Waters Corp., Milford, MA) operated from its front panel; the second dimension gradient was produced by a Waters 2795 liquid chromatograph controlled by the mass spectrometer software.

The mobile phases used for the strong cation exchange dimension were 6 M urea with 20 mM methylammonium acetate (pH 5.00, SCX A) and 6 M urea, 500 mM NaCl with 20 mM methylammonium acetate (pH 5.00, SCX B). The reversed phase dimension employed 5% (v/v) acetonitrile in 0.1% (v/v) aqueous formic acid (RP A) and 5% (v/v) water, 0.1% (v/v) formic acid in acetonitrile (RP B). The SCX and RP flow rates were 300 and 50 μL/min, respectively; the gradient programs were similar to those presented in Tables 1 and 2. The trapping columns' short length allowed them to be placed in line with the SCX column with a system pressure of 2100 psi at 300 μL/min).

### 3.4. 60-Trap system design

Fig. 1 is a block diagram of the fluid connections in the 60-trap system. The gradients for the two separations were provided

Table 1  
Strong cation exchange gradient for 60-trap separation

| Time (min) | Percent SCX B | Slope               |
|------------|---------------|---------------------|
| 0          | 0             | Step <sup>a</sup>   |
| 5          | 10            | Step                |
| 25         | 35            | Linear <sup>b</sup> |
| 26         | 35            | Linear              |
| 75         | 70            | Linear              |
| 76         | 100           | Linear              |
| 82         | 100           | Linear              |
| 83         | 0             | Step                |
| 90         | 0             | Step                |

<sup>a</sup> Step gradients change the solvent composition instantaneously at the specified time.

<sup>b</sup> Linear gradients change the solvent composition in a linear fashion between the specified times.

by the two liquid chromatographs specified above; a Beckman model 110A pump (Beckman-Coulter Inc., Fullerton, CA) regenerated the two analytical columns by providing a constant flow of RP A. Valve A selected which of the two chromatographs were inline with the traps. Valve 6 directed the flow into one of six 10-position column selection valves (valves 0–5) and then into valve B; the trapping columns were attached to the ports on valves 0–5. Valve B sent the effluent from the traps either to waste or to valve C thereby isolating the mass spectrometer from the salts and urea used in the SCX separation. Valve C directed the effluent from the traps onto one of two C<sub>4</sub> analytical columns. The analytical column receiving effluent from the traps was connected to the source of the mass spectrometer; the Beckman pump pushed approximately 100 μL/min of RP A through the other analytical column. All valve movements were controlled by a Labview program (version 6.0, National Instruments, Austin, TX). The table of valve positions throughout the experiment was created in Microsoft Excel, and the Labview program used this table to control the valves via RS-485. The entire system was synchronized using contact closures from the two HPLC pumps.

### 3.5. ESI-QTOF mass spectrometry

The masses of proteins were measured by a QTOF Micro quadrupole/time-of-flight (QTOF) mass spectrometer (Waters) equipped with an electrospray ionization (ESI) source; the spectrometer was controlled by MassLynx 4.0 (Waters). A passive

Table 2  
Reversed phase gradient table for the 60-trap separation

| Time (min) | Percent RP B | Slope  |
|------------|--------------|--------|
| 0          | 0            | Step   |
| 7          | 0            | Linear |
| 7.1        | 20           | Linear |
| 37         | 70           | Linear |
| 40         | 90           | Linear |
| 44         | 90           | Linear |
| 44.1       | 0            | Linear |
| 53         | 0            | Linear |

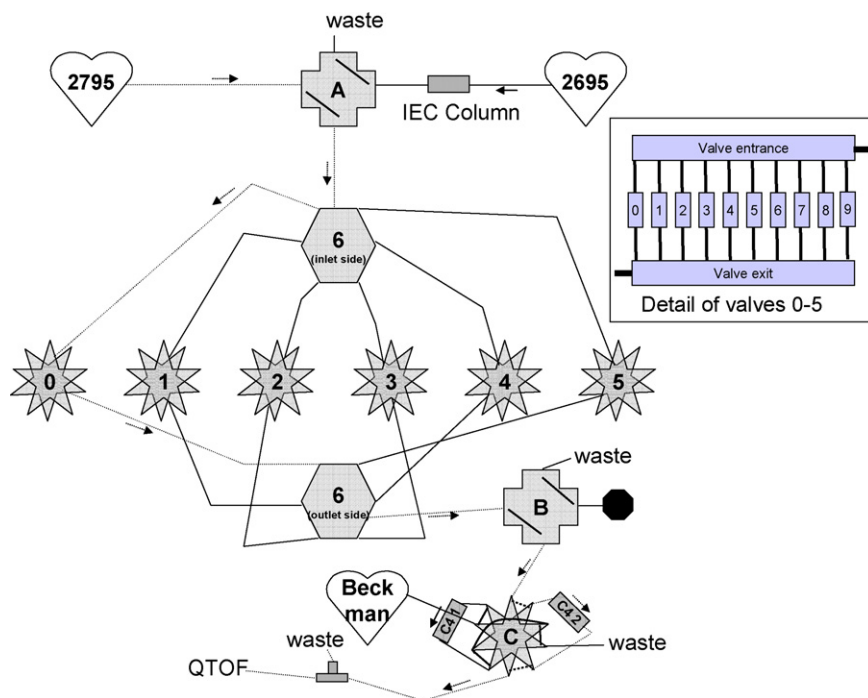


Fig. 1. Block diagram for the 60-trap system (all 2 position valves in position A). Gray polygons represent the valves, the heart shapes correspond to the three pumps in the system. The numbers inside the polygons refer to the valve labels described in the text. The rectangles are the SCX and analytical C<sub>4</sub> columns. A trapping column is attached to each point of the 10-sided polygons as shown in the inset.

flow-splitter directed 5  $\mu\text{L}/\text{min}$  into the mass spectrometer; the remainder was either sent to an off-line fraction collector or discarded. Positive ion mass spectra were recorded from  $m/z$  600 to 1800 and each scan was a one second integration; the interscan delay was 0.1 s. One microlitre of deionized water was injected at the beginning of each reversed phase separation to define its start time. Data were recorded for 40 min, starting 10 min into the RP gradient.

### 3.6. ESI-TOF data analysis

ESI-TOF mass spectral charge distributions were deconvoluted using either the MaxEnt 1 [53] subroutine of MassLynx 4.0 or ProTrawler [54] (BioAnalyte Inc., Portland, ME). The MaxEnt 1 parameters were: output spectrum range from 4000 to 40,000 Da at a resolution of 1 Da, a 0.75 Da wide peak was assumed for each member of a charge state distribution, and the algorithm performed up to 25 iterations. A macro called AutoME (Automated MaxEnt) was used to process batches of QTOF chromatograms. AutoME combined 100 scan wide segments of each chromatogram and automatically called MaxEnt 1 to deconvolute ion distributions. The ESI-TOF data were recorded at approximately 55 scans per minute, thus 100 scans correspond to about two minutes of chromatographic retention time. AutoME required approximately 20 hours to perform the 300 deconvolutions in a 20 trap data set. ProTrawler deconvoluted 30-scan segments of the QTOF data using one of four charge state distribution molecules (based on proteins with molecular weights of 7.1, 12.3, 20.8, and 28.0 kDa). Each model was used to produce an output spectrum from 0.5 to 2 times the

molecular weight of the protein on which it was based (e.g. 6–24 kDa for the analysis with the 12.3 kDa model). ProTrawler required approximately 10 h to complete all 3360 analyses for a 20 trap experiment. ProTrawler's four output files from each chromatogram were reconciled into a single output table with masses ranging from 4.0 to 56 kDa with the Regatta software package from BioAnalyte. Many protein masses were observed in more than one deconvoluted spectrum and all masses reported in this document are intensity-weighted averages.

### 3.7. Data presentation

The volume of data generated by these two systems created challenges in information management and presentation. A 60-trap separation generated nearly 7 GB of raw data that grew to 10 GB after MaxEnt 1 processing. Two different data presentation solutions have been presented in the literature. Liu et al. combined their total ion chromatograms (TICs) end-to-end to form one long chromatogram in which overall retention time indicated retention in both dimensions [43]. Lubman and coworkers used 2-D image plots to present their data [31,32,34,35]. The vertical and horizontal axes in their images represented the elution time from the two separations and color (or brightness in a gray-scale plot) corresponded to intensity. The Lubman group also created "virtual 2-D gels" in which the horizontal dimension corresponded to isoelectric point and the vertical dimension was intact protein mass [55]. A significant advantage of 2-D image plots is that they appear very similar to the images obtained from 2-dimensional gels. Figs. 4–7 were created using OriginPro 7.0 (OriginLab Corp.,



Northampton, MA) to display data processed with MaxEnt 1. The vertical dimensions in these plots correspond to retention time in the reversed phase dimension, while each column is a single reversed phase chromatogram from a different trap. The horizontal dimension correlates with ion exchange retention time. TIC data from the reversed phase separations were manually copied from MassLynx into OriginPro for conversion. Fig. 8 was created by Regatta directly using the “1-D gel” function. It is important to note that each TIC in the image plots was individually normalized to prior drawing the figure. Without this step, the image plots appeared as black backgrounds with one or two bright white spots and a handful of very dark gray spots. Normalization did remove much of the quantitative information and introduced some artifacts. Some of these normalization artifacts are explored below. Furthermore, because different proteins are ionized and detected with varying efficiencies, it is not standard practice to quantitate proteins directly from their mass spectrometric intensities. Most mass spectrometric quantitation schemes for biological samples involve stable isotope labeling and relative abundance measurements [56].

## 4. Results and discussion

### 4.1. Trapping column validation

One of the first questions that had to be answered was how well proteins could be recovered from the trapping columns after several hours of storage. This issue was studied by performing replicate analyses on samples that had been allowed to sit adsorbed on trapping columns for varying amounts of time. A mixture of four proteins (1.0  $\mu\text{g}$  each of horse cytochrome C, bovine carbonic anhydrase, ovalbumin, and bovine serum albumin) was injected onto a trapping column and buffer RP A was washed over them for five minutes. The flow of solvent was stopped for varying amounts of time to simulate what would happen as adsorbed SCX fractions sat waiting for reversed phase analysis. After the delay, the solvent flow was restarted and the proteins eluted with a short gradient. Fig. 2 displays the UV-absorption (280 nm) chromatograms from four of these separations. The four traces look remarkably similar. The broad features at the beginning of each delay trace were caused by small air bubbles that formed in the detector when the solvent flow was stopped. Clearly, storing proteins on C<sub>4</sub> columns

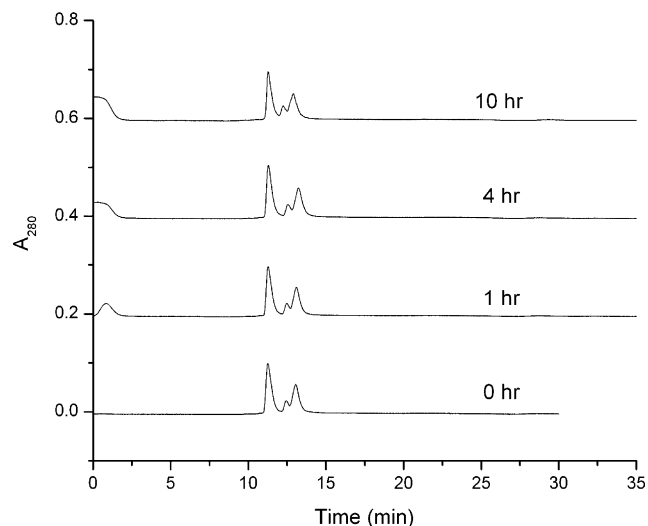


Fig. 2. Absorbance chromatograms (280 nm) from repeated separations of a four protein mixture. The times in the chromatogram labels refer to the length of the delay between loading of the sample and the start of the gradient.

for long periods did not significantly alter their separation characteristics.

An obvious question about this apparatus is how many traps to use. Too few traps limit the resolution of the first dimension separation while individual proteins will be observed in several different fractions if too many traps are used. Fig. 3 is a chromatogram obtained by separating 150  $\mu\text{g}$  of *Caulobacter* ribosomal proteins using the Tosoh SCX column. The peaks are approximately 1.5 min wide, so fractionating the proteins into 60 traps over 90 min appears reasonable.

A third concern is absolute recovery of material from the various chromatographic columns. A series of experiments probed this facet of the system. 100  $\mu\text{g}$  each of lysozyme and  $\alpha$ -chymotrypsinogen were loaded onto the ion exchange column and eluted with the gradient used in the ribosome separation. A nearly 90% recovery was estimated by Bradford assay [52]. Separation of 30  $\mu\text{g}$  each of lysozyme, myoglobin, and  $\alpha$ -chymotrypsinogen on the trap-analytical column combination revealed a 117% recovery by Bradford assay. A 118% recovery estimate was obtained by pooling all fractions from a separation of 100  $\mu\text{g}$  of ribosomes onto 20 traps followed by C<sub>4</sub> reversed phase HPLC. The greater than 100% recovery may arise from

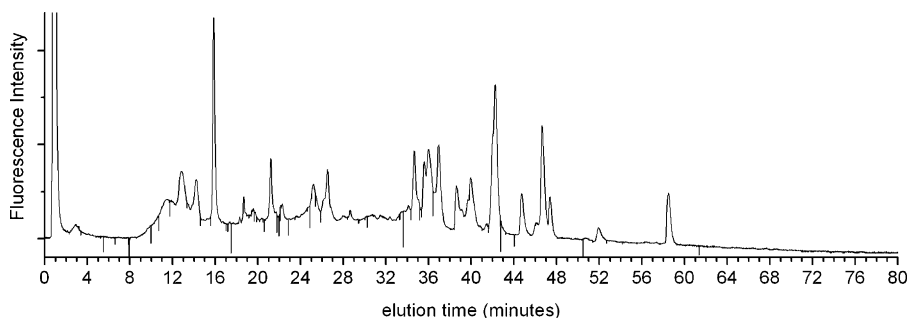


Fig. 3. Fluorescence chromatogram from 150  $\mu\text{g}$  injection of ribosomes onto a TSKGel SCX column. The excitation wavelength was 280 nm; the fluorescence emission wavelength was 350 nm.



Table 4  
Reversed phase gradient table for the triplicate 20-trap separation experiments

| Time (min) | Flow rate ( $\mu\text{l}/\text{min}$ ) | Percent RP B |
|------------|--|--------------|
| 0          | 50                                     | 0            |
| 7          | 50                                     | 0            |
| 7.1        | 50                                     | 20           |
| 37         | 50                                     | 70           |
| 40         | 50                                     | 90           |
| 44         | 50                                     | 90           |
| 44.1       | 50                                     | 0            |
| 53         | 50                                     | 0            |

All slopes were linear.

tionated as follows: trap 1 for the first 10 min, trap 2 for the next 10 min, 5 min each in traps 3–19, with the final 10 min of the gradient directed through trap 20. The retention times in both dimensions were highly reproducible. The relative standard deviations (RSDs) of the second dimension retention times ranged from 0.1 to 0.7% for 10 randomly selected proteins. It should be noted that these data correspond to proteins separated on the same analytical column (C4 1 or C4 2 in Fig. 1) as the two analytical columns had slightly different retention characteristics; this phenomenon is discussed below. We also studied the observed intensities of the proteins as they eluted from the system. The intensities of protein ions are not normally used for quantitative purposes due to the large number of experimental variables (e.g. source conditions, elution solvent composition, and ionization/detection efficiencies). Table 5 lists the observed intensities in the three experiments for 10 different ribosomal subunit proteins. There was no overall pattern to the intensity data. None of the three separations gave low intensities for all proteins. In fact the low intensity results are rather evenly distributed (three in traps 1–20, four each in traps 21–40 and 41–60). Furthermore, the intensities of the proteins varied over nearly two orders of magnitude. These results underscore the fact that different proteins are ionized and detected with different efficiencies. Therefore, care must be taken when deriving quantitative information from protein mass spectrometry intensities alone.

Table 5  
Summed mass spectrometric intensities of 10 different ribosomal subunit proteins from the triplicate experiments

| Protein | mass   | area in traps 1-20 | area in traps 21-40 | area in traps 41-60 | RSD  |
|---------|--------|--------------------|---------------------|---------------------|------|
| L36     | 4,832  | 6.35E+04           | 7.87E+04            | 9.54E+04            | 20.1 |
| L32     | 6,794  | 6.63E+05           | 7.43E+05            | 5.98E+05            | 10.8 |
| L31     | 8,376  | 3.21E+05           | 3.67E+05            | 3.22E+05            | 7.8  |
| L24     | 10,865 | 1.12E+06           | 6.25E+05            | 1.24E+06            | 32.8 |
| S12     | 13,694 | 1.19E+05           | 4.57E+05            | 3.51E+05            | 55.8 |
| S6      | 14,434 | 3.05E+06           | 2.57E+06            | 2.82E+06            | 8.5  |
| L10     | 18,040 | 9.83E+05           | 2.38E+06            | 1.95E+06            | 40.4 |
| S5      | 21,498 | 1.94E+06           | 1.54E+06            | 1.75E+06            | 11.6 |
| L3      | 26,667 | 1.34E+05           | 5.30E+04            | 1.50E+05            | 46.3 |
| S3      | 28,013 | 5.09E+05           | 9.21E+05            | 4.07E+05            | 44.4 |

The relative standard deviations (RSDs) are given in percent. The lowest intensity for each protein is highlighted.

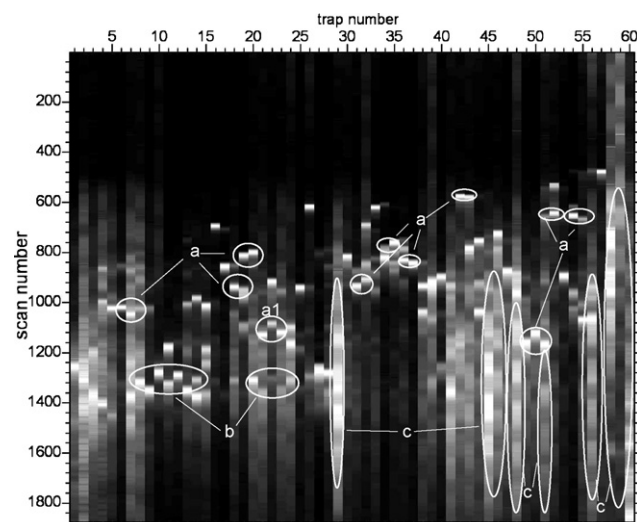


Fig. 6. Image plot of data from separation of a 100  $\mu\text{g}$  *Caulobacter* ribosome sample on the 60-trap system. Each TIC was independently normalized prior to plotting. Labeled ellipses are explained in the text.

#### 4.3. 60-Trap system characterization

The full 60-trap device was tested by separating 100  $\mu\text{g}$  of *Caulobacter* ribosomal proteins. The SCX effluent was directed into a different trap every 90 s throughout the first dimension separation. It is important to note that the gradient for the first dimension separation was set up to maximize peak capacity (i.e. have proteins elute into as many different traps as possible). Fig. 6 contains the 2-D image plot of the TIC data. Although the features are too small to label as in Figs. 4 and 5, several features stand out. The first is the large number of bright bands observed in almost every trap. Protein signals were observed only in traps 1–14 in the 20 trap experiments (see Figs. 4 and 5); proteins were observed in traps 4–57 in the 60 trap separation.

An important criterion for assessing the 60-trap system's performance was whether the number of traps was appropriate for the peak capacity of the SCX separation. Splitting the same protein into multiple traps causes an undesirable reduction in sensitivity. Conversely, the number of traps must be sufficient to exploit the peak capacity of the first dimension separation. It was clear that 20 traps were not quite adequate to fractionate the ribosomal proteins as several of them coeluted in Figs. 4 and 5 (e.g. L3 and L19 or S12 and S13). Fig. 6 suggests that about half of the proteins eluted in primarily one trap and half eluted in two or three traps. Examples of the latter are circled and labeled with an "a" in Fig. 6. A protein was observed in two traps when the system switched while it was eluting off of the SCX column. Since a few proteins were observed in three traps and a significant number were observed in two traps, it is apparent that the number of traps slightly exceeds the peak capacity of the SCX separation.

One would expect the retention time of a protein to remain nearly unchanged every time it was separated on the same type of column with the same gradient. That would appear as a solid white/gray bar 2 columns wide in Fig. 6. The circle labeled "a1" in Fig. 6 envelops three chromatographic features whose mass

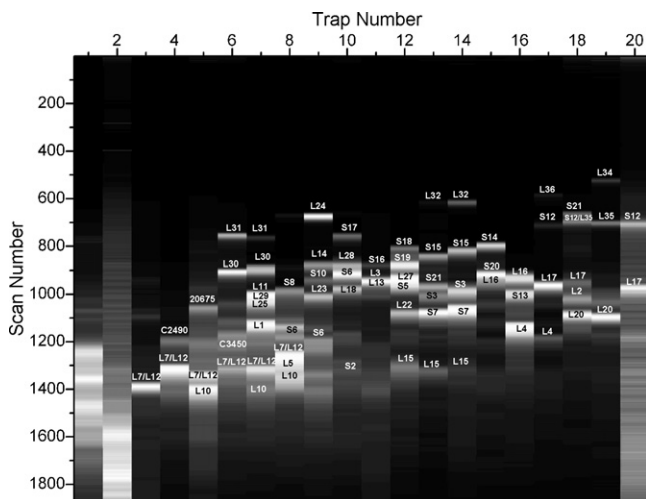


Fig. 7. 2-D image plot of intensity as a function of trap number and scan number (reversed phase retention time) for one of the triplicate separations of 125  $\mu\text{g}$  of *Caulobacter* ribosomal proteins.

spectra indicate ribosomal subunit protein S6. The three bands alternate in vertical position. Comparable shifts are observed for all bands labeled “a” in Fig. 6. The shifts in the positions of the S6 bands correspond to 0.8 min variations in reversed phase retention time. In this experiment, all even-numbered traps eluted through column “C4 1” and all odd-numbered traps through column “C4 2” (see Fig. 1). The data in Fig. 7 show proteins were retained slightly longer in the odd-numbered traps indicating a difference in the retentiveness of the two analytical columns connected to Valve C. One possible solution to this problem is removing the analytical columns from the system and using the traps as analytical columns. It is known that column length does not have a large impact on resolution in reversed phase separations of proteins [59]. One concern is that the proteins would diffuse from the heads of the later-developed trapping columns during the nearly 50 h required to complete an experiment, leading to broad peaks in the TICs. The data in Fig. 2 suggest this might not be much of a problem. The analytical columns were placed after the traps to minimize any peak broadening that occurred during the time between the two separations, and many systems employing online trapping columns use this arrangement [45–49]. Optimal matching of the two columns may not fully alleviate this problem as the performance of the two columns might degrade at different rates.

The regions labeled “b” in Fig. 6 correspond to portions of the data whose deconvoluted spectra contained a feature at 13,172 Da, which is consistent with ribosomal subunit protein L7/L12. A large number of peaks consistent with L7/L12 were observed in the 20-trap experiments as well. L7 and L12 are intriguing in that they have the same sequence. In *E. coli*, L7 retains its N-terminal methionine and is acetylated, while L12 loses its N-terminal methionine and is methylated [60]. The form of L7/L12 most commonly observed in these experiments had lost its N-terminal methionine and was methylated, corresponding to L12, although much smaller amounts of acetylated L7 were also observed. In *E. coli*, there are two copies of L7 and two copies of L12 in each ribosome; only one copy of each of the

other ribosomal subunit proteins is found in a single ribosome [57]. It is possible that the poor focusing of L7/L12 during the SCX separation results from non-denatured multimers or differently folded versions of L7/L12. This is further considered in a separate publication [58].

No protein signals were observed in the total ion chromatograms from the first three and last two traps, nor remarkably, in any of the regions labeled “c” in Fig. 6. The bright areas in those regions correspond to increases in background chemical noise. Each TIC was individually normalized by dividing all intensities in a TIC by the largest one, and the brightness of some areas associated with little protein signal are data processing artifacts. That is, if no proteins eluted from a particular trap, then background noise is the basis for the normalization, and it appears abnormally bright in the image plot. Areas circled and labeled “c” in Fig. 6 display intensity patterns that look somewhat periodic. Intensity maxima appear approximately every three minutes in the TIC traces in which they are observed. A closer look at the raw data revealed a general increase in the TIC signal, but no discernable peaks. Deconvoluted spectra derived from these data were equally featureless. The origin of these weak and ill-defined features may be non-protein material eluting/bleeding off of the SCX or C4 columns.

A wider range of column dimensions and gradient conditions needs to be explored. The SCX separation was performed at a flow rate slightly below the optimum recommended in Tosoh’s literature in order to limit back pressures, and increasing the flow rate of the SCX gradient might improve the resolution in the first separation. Another aspect that could be improved is the concentration of analytes between dimensions. The current configuration incorporates a six-fold reduction in flow rate between the first and second separations. This concentration effect could be increased either by raising the flow rate in the first dimension or reducing the inner diameter of the trapping and analytical columns; the problem with either approach is back pressure. The Tosoh SCX column has a maximum recommended pressure drop of 3000 psi. Since the pressure drop across the SCX column was approximately 1700 psi, there is some room for flow-rate increase and little danger in a slight reduction in trapping column diameter. One solution that would allow even higher back pressure is to switch SCX stationary phases to a more robust substrate (e.g. silica or zirconia). The methacrylate beads in the Tosoh column provide excellent chemical resistance, however, and columns packed with this material can be used in buffer conditions that would destroy most silica-based stationary phases (e.g. anion exchange experiments at pH >7). Another issue in column selection is loading capacity; the reported loading capacity for the Tosoh column is only 200  $\mu\text{g}$ , approximately the same as an analytical-scale 2-D gel. A significantly larger capacity is needed in order to work on the semi-preparative scale required to isolate low-copy number proteins [19,20].

Another question concerning peak capacity is how often two proteins co-elute in this system. The ribosome contains only 54 separate subunit proteins, and is not complex enough to fully explore this concern. Fig. 4 reveals six pairs of co-eluting proteins (L10 and S2, L3 and L19, L13 and S19, S7 and L21, S12 and S13, L17 and L16). Clearly, co-elution becomes more



problematic as sample complexity increases. The mass spectrum represents a third dimension that can be exploited to distinguish co-eluting proteins (e.g. L10 and S2 have masses of 18,040 and 28,012 Da, respectively). Similar problems occur in any scheme used to separate complex mixtures, and researchers must often use additional separations to resolve co-eluting species.

In its present configuration, the apparatus described herein offers no significant speed advantage over 2-D gel electrophoresis. The bulk of the analysis time is spent on the second dimension separations, thus optimization of these could considerably shorten the experiment. The system described recorded mass spectra for 40 min during each 50 min reversed-phase gradient. Optimization of the HPLC gradient (e.g. cutting seven or eight minutes of desalting time from the gradient and starting at a higher percentage of RP B) could remove several hours from the experiment. Unfortunately, some of the inefficiency in the separation was due to the 2795 pump itself. The Waters 2795 is a low pressure mixing, analytical scale chromatograph with nearly 450  $\mu\text{L}$  of void volume between the gradient proportioning valve and the head of the column (nine minutes at 50  $\mu\text{L}/\text{min}$ ). The relatively large void volume clearly delays the gradient arrival on the traps and reversed phase columns. Much of this void volume could be removed if pumps with high pressure mixing at the column head were employed. Alternatively, a splitter right in front of the columns would allow the 2795 to operate at a much higher flow rate, minimizing the impact of the void volume. The 5  $\mu\text{m}$ , porous, reversed-phase particles in the traps and analytical columns could be replaced with more efficient stationary phases (e.g. 1.5  $\mu\text{m}$  non-porous particles, 1.8  $\mu\text{m}$  ultra-high pressure porous particles, or monolithic stationary phase). If the reversed phase analysis time could be reduced to 15 min, the complete two-dimensional separation could be completed in 17 h, not 60. These changes and others will be explored in the future.

A complex issue associated with the current system is data presentation and management. The 60-trap experiment generated nearly 10 GB of data after MaxEnt 1 processing. Each deconvoluted mass spectrum contained 56,000 data points, and there were 900 of these totaling over 50 million data points. The image plots in Figs. 4–6 were created from the total ion chromatogram traces, ignoring all mass information. A plot of intensity as a function of trap number and molecular weight should be able to resolve the coeluting species in Fig. 7. The Regatta software package facilitated plotting molecular weight as the vertical dimension instead of retention time. Fig. 7 is the 2-D plot for one of the triplicate analyses described above using scan number (reversed phase retention time) on the vertical axis and looks very similar to Figs. 4–6. Fig. 8 is a plot of the same data but the vertical axis is now molecular weight as determined by the mass spectrometer. Assuming no additional modifications, a protein's molecular weight is independent of its retention time. Utilizing molecular weight as the vertical dimension eliminates the retention time differences observed when a protein elutes into two different traps as seen in Figs. 4–7. In Fig. 7, proteins L11, L29, and L25 coelute in trap 7, but are clearly resolved in Fig. 8. Similarly, in Fig. 8, proteins S6 and S8 appear to coelute in trap 8, but they are clearly resolved in Fig. 7. The inset of Fig. 8 highlights the resolution of the ESI-

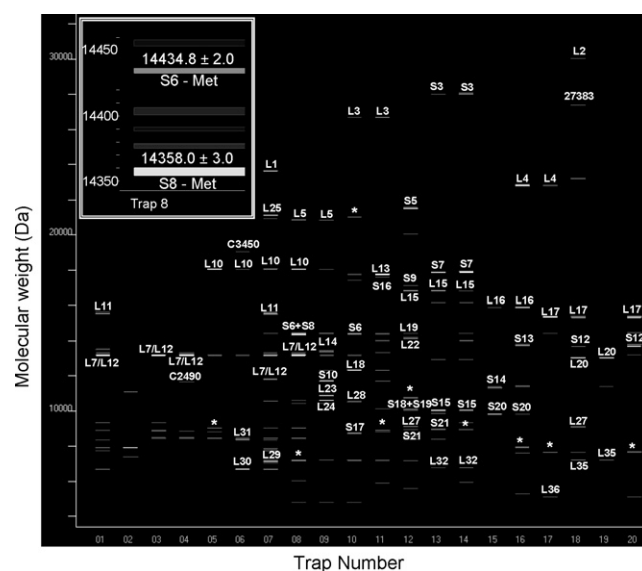


Fig. 8. 2-D image plot of intensity as a function of trap number and deconvoluted molecular weight for one of the triplicate separations of 125  $\mu\text{g}$  of *Caulobacter* ribosomal proteins. The inset expands a portion of the data from trap 8. The asterisks indicate features arising from artifacts of the deconvolution process. Only those features with more than 5% relative intensity in each trap are shown.

QTOF mass spectrometer. The dark gray features accompanying proteins S6 and S8 correspond to oxidized (+16 and +32 Da) and sodiated (+22 and +44 Da) versions of the proteins. In fact, all species that appeared to co-elute in Fig. 8 were resolvable when the vertical scale of was expanded. Figs. 7 and 8 convey complementary information and both plot types (molecular weight and retention time) contribute to a complete analysis. Retention time plots are needed to assess the performance of the chromatography and determine which fractions contain proteins that need further analysis while the molecular weight plots convey the information required for protein identification and to elucidate co-eluting features.

An improved software solution would allow the creation of image plots using any combination of trap number, reversed phase retention time, and deconvoluted protein mass and keep track of annotation information (e.g. protein identities, modifications, etc.). One could use deconvoluted mass information to look for all occurrences of a specific protein mass (e.g. L12 at 13,172 Da) to create an image plot with only one or two bright areas. These areas would correspond to a particular mass spectral feature facilitating the isolation of a specific version of a protein (e.g. highlight a particular modified protein). A 3-dimensional plot of these data (e.g. trap number in the X dimension, reversed phase retention time in the Y dimension, protein mass in the Z dimension, and intensity represented with a color scale) would be helpful if the proper tools existed to interact with all the data (e.g. ability to rotate the plot freely in all three dimensions and quickly obtain mass or retention time information for a particular feature). The issue of the normalization of each TIC (employed mainly for aesthetic reasons) needs to be addressed if quantitative information is to be obtained from this apparatus.

The asterisks in Fig. 8 label bands that correspond to artifacts of the deconvolution process. The molecular weight for

ribosomal subunit protein L10 (trap 5) is 18,040 Da (no modifications observed), but the deconvoluted mass spectrum contained features at 18,040 and 9020 Da; 9020 is exactly one-half of 18,040. Similar observations were made for ribosomal subunit proteins S6 (trap 8), L13 (trap 11), S7 (trap 14), L4 (trap 16), and L17 (trap 17). Likewise, the intact molecular weight of ribosomal subunit protein L28 (trap 10) is 10,499 Da (loss of N-terminal Met [58]), yet its deconvoluted mass spectrum had features at 10,499 and 20,999 Da. Usually the artifact peaks were less intense than the feature corresponding to the actual protein, but the 21 kDa feature was slightly more intense than the 10.5 kDa peak in the ProTrawler data (trap 10). MaxEnt 1 data occasionally generated higher “harmonics” (three or four times the correct molecular weight). The artifacts arise because the predicted charge state distributions for species at integral ratios of a protein’s molecular weight (e.g. 1:2, 2:1, 3:1) are very similar. For example, the predicted +14, +15, +16, +17, and +18 charge states of a protein of mass 18,040 have  $m/z$  ratios of 1289.6, 1203.7, 1128.5, 1062.2, and 1003.2, respectively, and the +7, +8, and +9 charge states of a 9020 Da protein are 1289.6, 1128.6, and 1003.2, respectively. These similarities are not correctly interpreted by automated deconvolution algorithms at present. A careful observer can quickly identify these artifacts when one compares the predicted charge state distribution with experimental data. For example, the L10 mass spectrum had very intense peaks at +14, +15, +16, +17, and +18, and the intensities of the +15 and +17 charge states were not explained by the suggested 9020 Da protein. Unfortunately such manual analysis is impractical when large volumes of data are processed. These artifacts have been briefly described before [54], and a more detailed study of these phenomena is ongoing.

## 5. Conclusions

A novel two-dimensional liquid chromatograph system was constructed and its performance characterized. The trapping columns in this apparatus were able to adsorb proteins from the ion exchange effluent and facilitate their desalting. Reversed phase resolution did not degrade due to long delays between the two separations. Intact protein masses were obtained by ESI-QTOF mass spectrometry. A subsequent publication will present all *Caulobacter* ribosomal protein assignments [58]. The 60-trap system described in this document is a flexible, robust separations platform that has been used by several other researchers.

The apparatus described functions as a sample preparation system, not a protein identification machine. An intact mass alone is rarely sufficient to identify a protein in a complex mixture. Traditional mass spectrometric protein identification methods relying on either enzymatic digest peptide masses [61,62] or sequence data obtained by tandem mass spectrometry [63–65] are still required to definitively identify the proteins separated by this apparatus. The 60-trap device will be coupled to a novel sample deposition and archiving apparatus [66] that will allow proteins separated by the 60-trap apparatus to be enzymatically digested prior to a second mass spectrometric analysis. The second mass spectrometer will facilitate both peptide mass mapping [67–71] and peptide ion fragmentation

experiments [63,64,72,73]. The combination of these technologies will enable comprehensive protein profiling of complex biological samples.

## Acknowledgements

This research was supported by National Science Foundation grant CHE0518234, the Indiana 21st Century Fund, and the Indiana Metacyte Initiative. We thank Dr. Ignatius Kass of Waters Corporation for the AutoME macro, the BioAnalyte Corporation for a development copy of Regatta, and Dr. Yves Brun for the initial culture of *C. crescentus*.

## References

- [1] W.C. Nierman, et al., Proc. Natl. Acad. Sci. U.S.A. 98 (2001) 4136.
- [2] F.R. Blattner, G. Plunkett III, C.A. Bloch, N.T. Perna, et al., Science 277 (1997) 1453.
- [3] R.D. Fleischmann, M.D. Adams, O. White, R.A. Clayton, et al., Science 269 (1995) 496.
- [4] F. Kunst, N. Ogasawara, I. Moszer, et al., Nature 390 (1997) 249.
- [5] J.P. McCormick, T. Thomason, J. Am. Chem. Soc. 100 (1978) 312.
- [6] J. Abelson, Annu. Rev. Biochem. 48 (1979) 1035.
- [7] F. Sherman, J.W. Stewart, S. Tsunasawa, Bioessays 3 (1985) 27.
- [8] D.L. Smith, Z.R. Zhou, in: J.A. McCloskey (Ed.), Methods in Enzymology, Academic Press, New York, 1990, p. 374.
- [9] H.T. Wright, Crit. Rev. Biochem. Mol. Biol. 26 (1991) 1.
- [10] T.E. Creighton, Proteins, Structure and Molecular Properties, W.H. Freeman and Company, New York, 1993, 49.
- [11] J.A. Kowalak, K.A. Walsh, Protein Sci. 5 (1996) 1625.
- [12] R.J. Arnold, B. Polevoda, J.P. Reilly, F. Sherman, J. Biol. Chem. 274 (1999) 37035.
- [13] C.S. Giometti, S.L. Tollaksen, G. Babnigg, C.I. Reich, G.J. Olsen, H. Lim, J.R. Yates III, Eur. J. Mass Spectrom. 7 (2001) 207.
- [14] A.-S. Petersson, H. Steen, D.E. Kalume, K. Caidahl, P. Roepstorff, J. Mass Spectrom. 36 (2001) 616.
- [15] Z. Zhang, D.L. Smith, J.B. Smith, Eur. J. Mass Spectrom. 7 (2001) 171.
- [16] R.J. Arnold, J.P. Reilly, in: C. Kannicht (Ed.), Posttranslational Modifications of Proteins: Tools for Functional Proteomics, Humana Press, 2002, p. 205.
- [17] S.-W. Lee, S.J. Berger, S. Martinovic, L. Tasa-Tolic, G.A. Anderson, Y. Shen, R. Zhao, R.D. Smith, Proc. Natl. Acad. Sci. U.S.A. 99 (2002) 5942.
- [18] B. Grunfelder, G. Rummel, J. Vohradsky, D. Roder, H. Langen, U. Jenal, Proc. Natl. Acad. Sci. U.S.A. 98 (2001) 4681.
- [19] G.L. Corthals, V.C. Wasinger, D.F. Hochstrasser, J.-C. Sanchez, Electrophoresis 21 (2000) 1104.
- [20] S.P. Gygi, G.L. Corthals, Y. Zhang, Y. Rochan, R. Aebersold, Proc. Natl. Acad. Sci. U.S.A. 97 (2000) 9390.
- [21] H.J. Issaq, T.P. Conrads, G.M. Janini, T.D. Veenstra, Electrophoresis 23 (2002) 3048.
- [22] S. Beranova-Giorgianni, Trends Anal. Chem. 22 (2003) 273.
- [23] S.-E. Ong, A. Pandey, Biomol. Eng. 18 (2001) 195.
- [24] V. Santoni, M. Molloy, T. Rabilloud, Electrophoresis 21 (2000) 1054.
- [25] A. Gorg, C. Obermaier, G. Boguth, A. Harder, B. Scheibe, R. Wildgruber, W. Weiss, Electrophoresis 21 (2000) 1037.
- [26] J.L. Harry, M.R. Wilkins, B.R. Herbert, N.H. Packer, A.A. Gooley, K.L. Williams, Electrophoresis 21 (2000) 1071.
- [27] H. Wang, S. Hanash, J. Chromatogr. B 787 (2003) 11.
- [28] E.P. Romijn, J. Krijgsveld, A.J.R. Heck, J. Chromatogr. A 1000 (2003) 589.
- [29] K.K. Unger, K. Racaiyte, K. Wagner, T. Miliotis, L.E. Edholm, R. Bischoff, G. Marko-Varga, J. High Resolut. Chromatogr. 23 (2000) 259.
- [30] D.B. Wall, M.T. Kachman, S.Y. Gong, R. Hinderer, S. Parus, D.E. Misek, S.M. Hanash, D.M. Lubman, Anal. Chem. 72 (2000) 1099.

- [31] D.B. Wall, M.T. Kachman, S.Y.S. Gong, S.J. Parus, M.W. Long, D.M. Lubman, *Rapid Commun. Mass Spectrom.* 15 (2001) 1649.
- [32] M.T. Kachman, H.X. Wang, D.R. Schwartz, K.R. Cho, D.M. Lubman, *Anal. Chem.* 74 (2002) 1779.
- [33] D.B. Wall, S.J. Parus, D.M. Lubman, *J. Chromatogr. B* 763 (2001) 139.
- [34] B.E. Chong, F. Yan, D.M. Lubman, F.R. Miller, *Rapid Commun. Mass Spectrom.* 15 (2001) 291.
- [35] F. Yan, B. Subramanian, A. Nakeff, T.J. Barder, S.J. Parus, D.M. Lubman, *Anal. Chem.* 75 (2003) 2299.
- [36] D.M. Lubman, M.T. Kachman, H. Wang, G. Siyuan, Y. Fang, R.L. Hamler, K.A. O'Neil, Z. Kan, N.S. Buchanan, T.J. Barder, *J. Chromatogr. B* 782 (2002) 186.
- [37] M.M. Champion, C.S. Campbell, D.A. Siegele, D.H. Russel, J.C. Hu, *Mol. Microbiol.* 47 (2003) 383.
- [38] B. Feng, A.H. Patel, P.M. Keller, J.R. Slemmon, *Rapid Commun. Mass Spectrom.* 15 (2001) 812.
- [39] G.J. Opticek, K.C. Lewis, R.J. Anderegg, J.W. Jorgenson, *Anal. Chem.* 69 (1997) 1518.
- [40] G.J. Opticek, K.C. Lewis, R.J. Anderegg, J.W. Jorgenson, *Anal. Chem.* 69 (1997) 2283.
- [41] G.J. Opticek, S.M. Ramirez, J.W. Jorgenson, A.M. Moseley III, *Anal. Biochem.* 258 (1998) 349.
- [42] K. Wagner, T. Miliotis, G. Marko-Varga, R. Bischoff, K.K. Unger, *Anal. Chem.* 74 (2002) 809.
- [43] H. Liu, S.J. Berger, A.B. Chakraborty, R.S. Plumb, S.A. Cohen, *J. Chromatogr. B* 782 (2002) 267.
- [44] M.P. Washburn, D. Wolters, J.R. Yates, *Nat. Biotechnol.* 19 (2001) 242.
- [45] M.T. Davis, J. Beierle, E.T. Bures, M.D. McGinley, J. Mort, J.H. Robinson, C.S. Spahr, W. Yu, R. Luethy, S.D. Patterson, *J. Chromatogr. B* 752 (2001) 281.
- [46] J. Chen, B.M. Balgley, D.L. DeVoe, C.S. Lee, *Anal. Chem.* 73 (2003) 3145.
- [47] E. van der Heeft, G.J. ten Hove, C.A. Herberts, H.D. Meiring, C.A.C.M. van Els, P.J.M. de Jong, *Anal. Chem.* 70 (1998) 3742.
- [48] B. Devreese, F. Vanrobaeys, J. Van Beeumen, *Rapid Commun. Mass Spectrom.* 15 (2001) 50.
- [49] L.J. Licklider, C.C. Thoreen, J. Peng, S.P. Gygi, *Anal. Chem.* 74 (2002) 3076.
- [50] G. Spedding, in: G. Spedding (Ed.), *Ribosomes and Proteins Synthesis: A Practical Approach*, IRL Press, Oxford, 1990, p. 1.
- [51] S.J.S. Hardy, C.G. Kurland, P. Voynow, G. Mora, *Biochemistry* 8 (1969) 2897.
- [52] S.M. Read, D.H. Northcote, *Anal. Biochem.* 116 (1981) 53.
- [53] A.G. Ferrige, M.J. Seddon, B.N. Green, S.A. Jarvis, J. Skilling, *Rapid Commun. Mass Spectrom.* 6 (1992) 707.
- [54] T.L. Williams, P.E. Leopold, S. Musser, *Anal. Chem.* 74 (2002) 5807.
- [55] N.S. Buchanan, R.L. Hamler, P.E. Leopold, F.R. Miller, D.M. Lubman, *Electrophoresis* 26 (2005) 245.
- [56] S.P. Gygi, B. Rist, S.A. Gerber, F. Turecek, M.H. Gelb, R. Aebersold, *Nat. Biotechnol.* 17 (1999) 994.
- [57] D.R. Benjamin, C.V. Robinson, J.P. Hendirck, F.U. Hartl, C.M. Dobson, *Proc. Natl. Acad. Sci. U.S.A.* 95 (1998) 7391.
- [58] W.E. Running, S. Ravipaty, J.A. Karty, J.P. Reilly, submitted for publication.
- [59] C. Flurer, C. Borra, F. Andreolini, M. Novotny, *J. Chromatogr.* 448 (1988) 73.
- [60] R.J. Arnold, J.P. Reilly, *Anal. Biochem.* 269 (1999) 105.
- [61] O.N. Jensen, M.R. Larsen, P. Roepstorff, *Proteins: Struct. Funct. Genet. Suppl.* 2 (1998) 74.
- [62] P. Jungblut, B. Thiede, *Mass Spectrom. Rev.* 16 (1997) 145.
- [63] J.K. Eng, A.L. McCormack, J.R. Yates III, *J. Am. Soc. Mass Spectrom.* 5 (1994) 976.
- [64] D.N. Perkins, D.J. Pappin, D.M. Creasy, J.S. Cottrell, *Electrophoresis* 20 (1999) 3551.
- [65] R.A. Zubarev, N.L. Kelleher, F.W. McLafferty, *J. Am. Chem. Soc.* 120 (1998) 3265.
- [66] K.S. Boraas, N.P. Christian, J.P. Reilly, 52nd ASMS Conference on Mass Spectrometry and Applied Topics, Nashville, TN, 2004.
- [67] W.J. Henzel, T.M. Billeci, J.T. Stults, S.C. Wong, C. Grimely, C. Watanabe, *Proc. Natl. Acad. Sci. U.S.A.* 90 (1993) 5011.
- [68] P. James, M. Quadroni, E. Carafoli, G. Gonnet, *Biophys. Biochem. Res. Commun.* 195 (1993) 58.
- [69] M. Mann, P. Hojrup, P. Roepstorff, *Biol. Mass Spectrom.* 22 (1993) 338.
- [70] D.J.C. Pappin, P. Hojrup, A.J. Bleasby, *Curr. Biol.* 3 (1993) 327.
- [71] J.R. Yates, S. Speicher, P.R. Griffin, T. Hunkapiller, *Anal. Biochem.* 214 (1993) 397.
- [72] R. Kaufmann, D. Kirsch, B. Spengler, *Int. J. Mass Spectrom. Ion Processes* 131 (1994) 355.
- [73] M.S. Thompson, W. Cui, J.P. Reilly, 52nd ASMS Conference on Mass Spectrometry and Applied Topics, Nashville, TN, 2004.